

Supporting Information

Tsygankov et al. 10.1073/pnas.0904405106

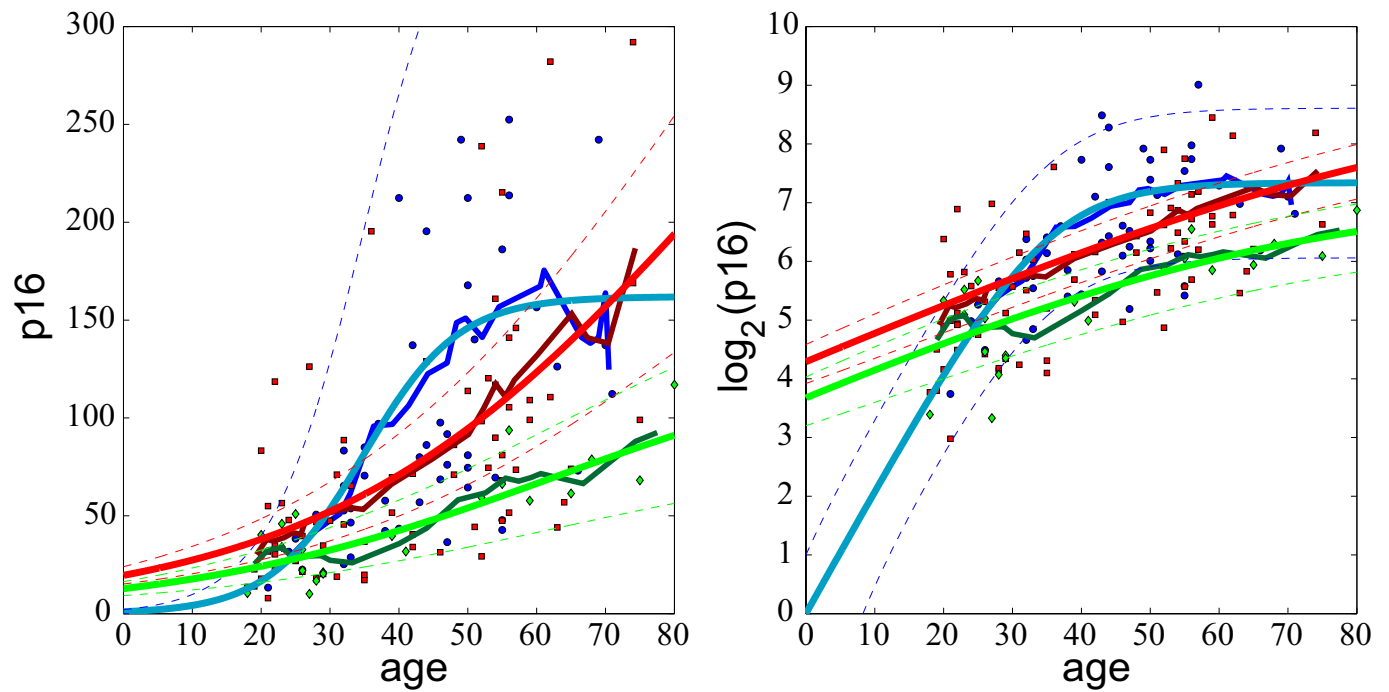


Fig. S1. Model II results for different genotypes (AA, blue; AG, red; GG, green). In this figure, the free parameters μ_0 (initial mean expression), u (growth rate), and d (death rate) are fit to the mean expression level. The parameters are $\mu_0 = 1$, $u = 0.14/\text{year}$ and $d = 0.0010/\text{year}$ for A/A, $\mu_0 = 19$, $u = 0.03/\text{year}$ and $d = 0.0016/\text{year}$ for A/G, and $\mu_0 = 13$, $u = 0.03/\text{year}$ and $d = 0.0034/\text{year}$ for G/G (see also parameters for Fig. 5). (Left) The data plotted on a linear scale. (Right) The same data plotted on log₂ scale. The standard deviations are plotted according to Eq. 3 in the main text with $\sigma_0 = \sqrt{\mu_0} = 2$.

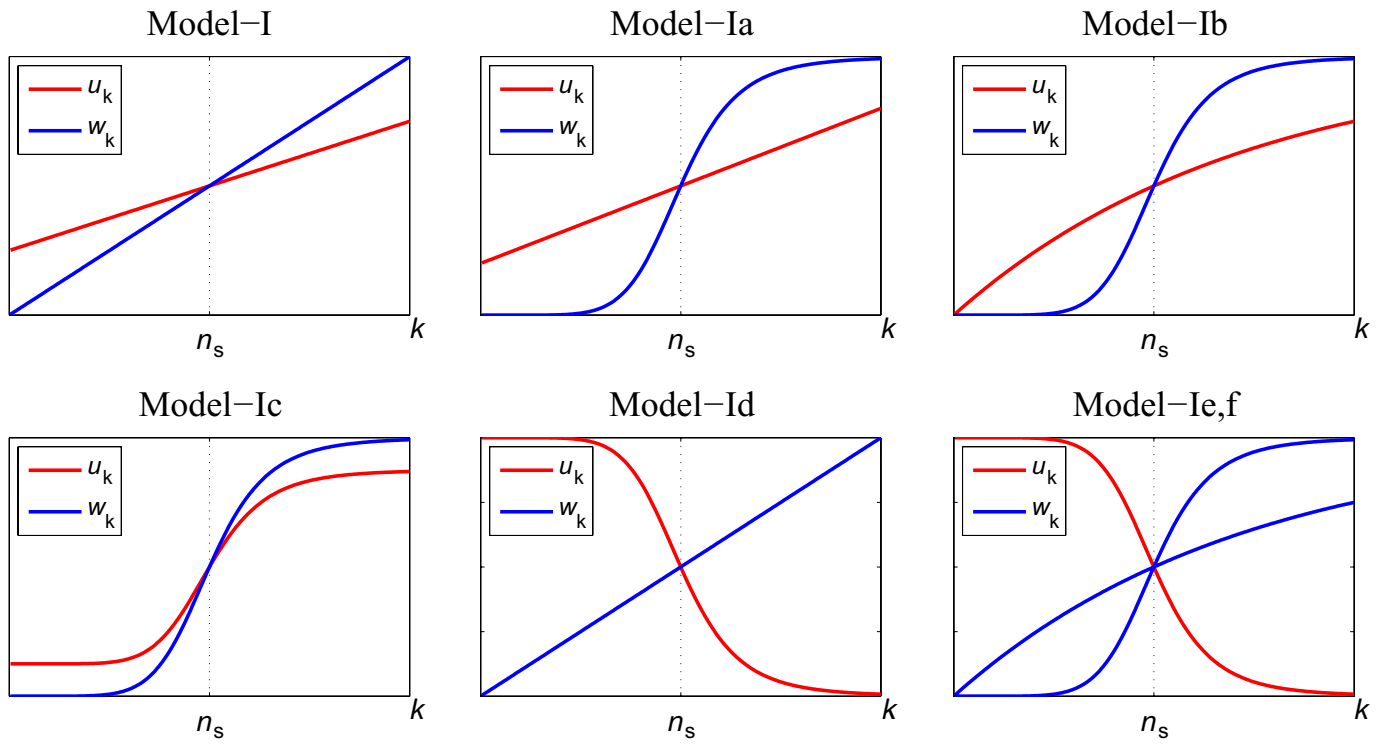


Fig. S2. Different examples from a class of down-regulation models that yield saturation at $k = n_s$. The red and blue curves are for the production rate, u_k , and degradation rate, w_k , respectively.

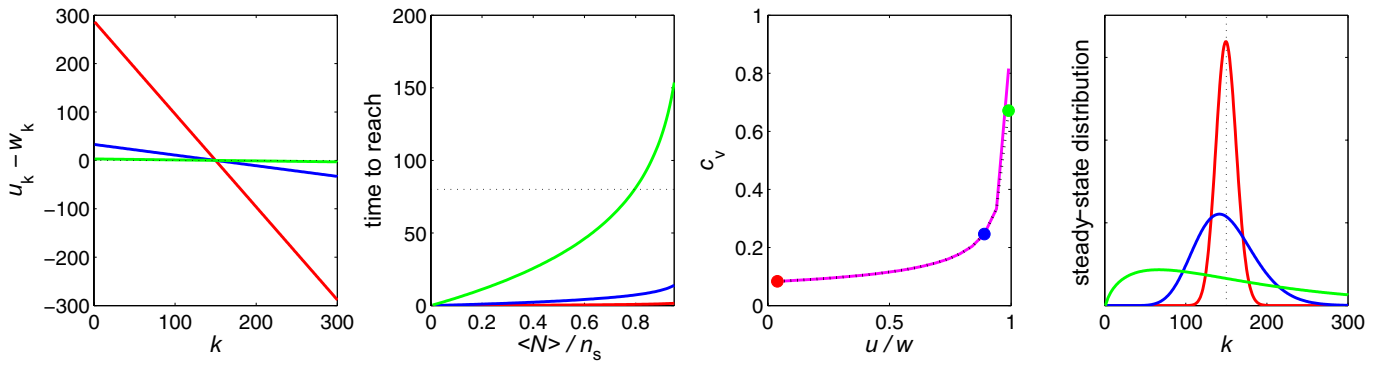


Fig. S3. Characteristics of the model I: (from left to right) the drift $u_k - w_k$, the time to reach $\langle N \rangle$, the steady-state coefficient of variation c_v as a function of the ratio u/w , and the steady-state distributions P_k . The dotted line in the second graph indicates 80 years. Red, blue, and green curves correspond to three different values of the ratio u/w as shown in the c_v graph. The black dotted curve in this graph is the exact solution, whereas the magenta curve is the approximation given by Eq. 29.

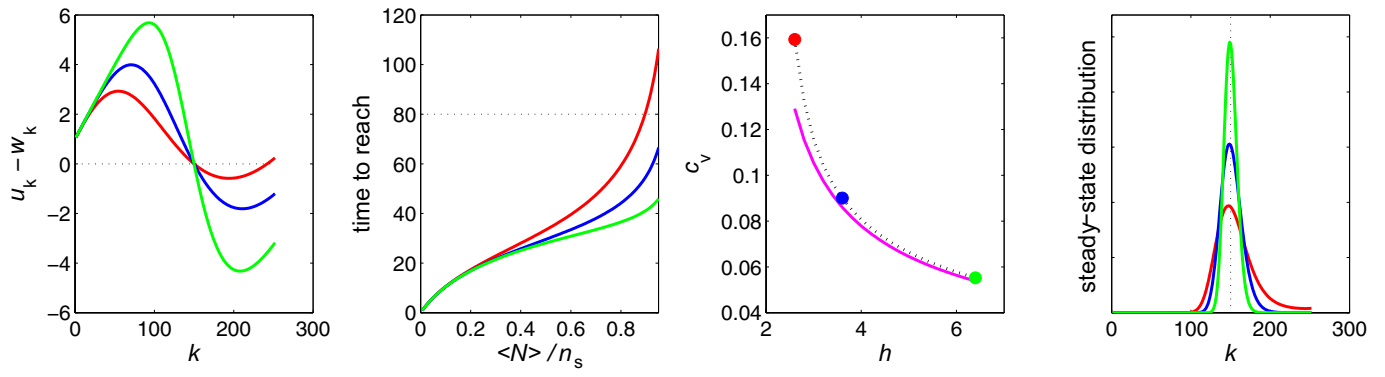


Fig. S4. The same as Fig. S3, but for the model Ia.

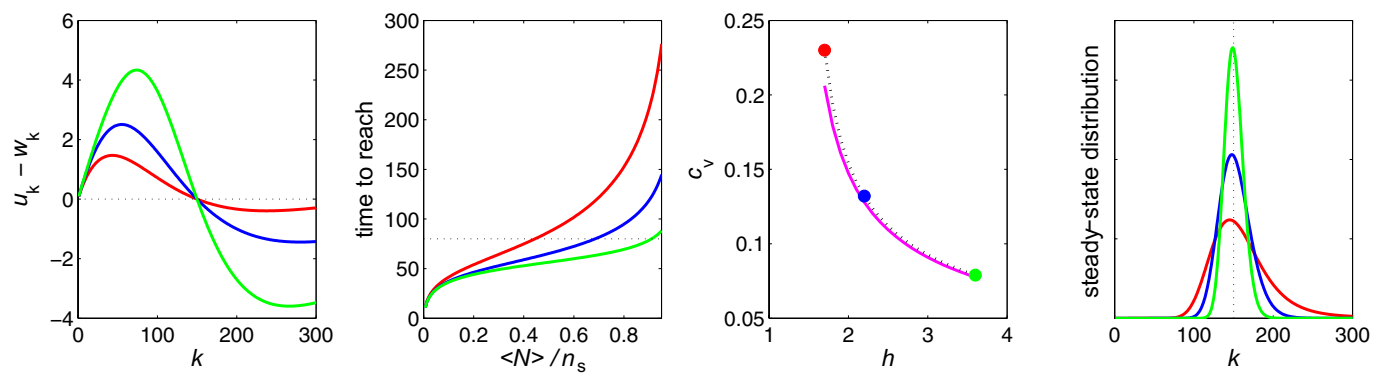


Fig. S5. The same as Fig. S3, but for the model 1b.

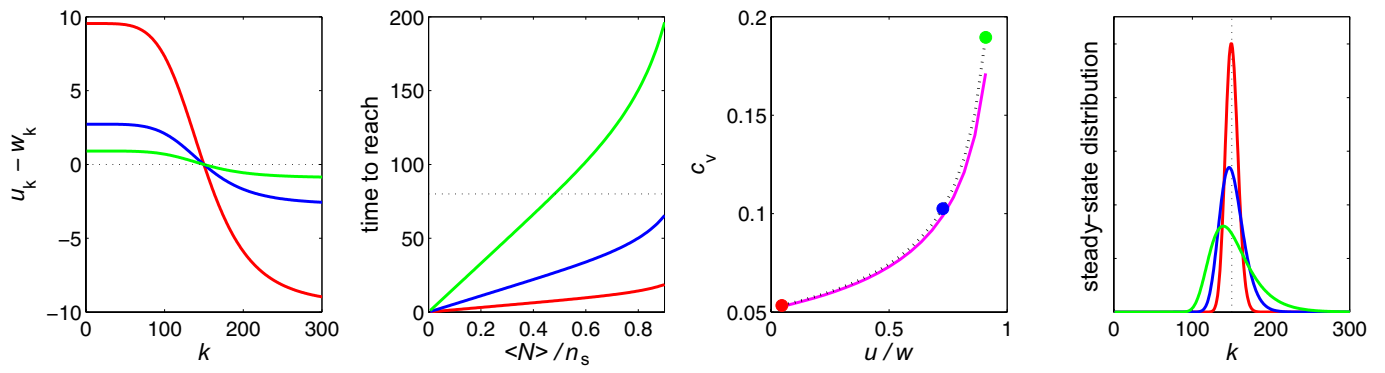


Fig. S6. The same as Fig. S3, but for the model Ic.

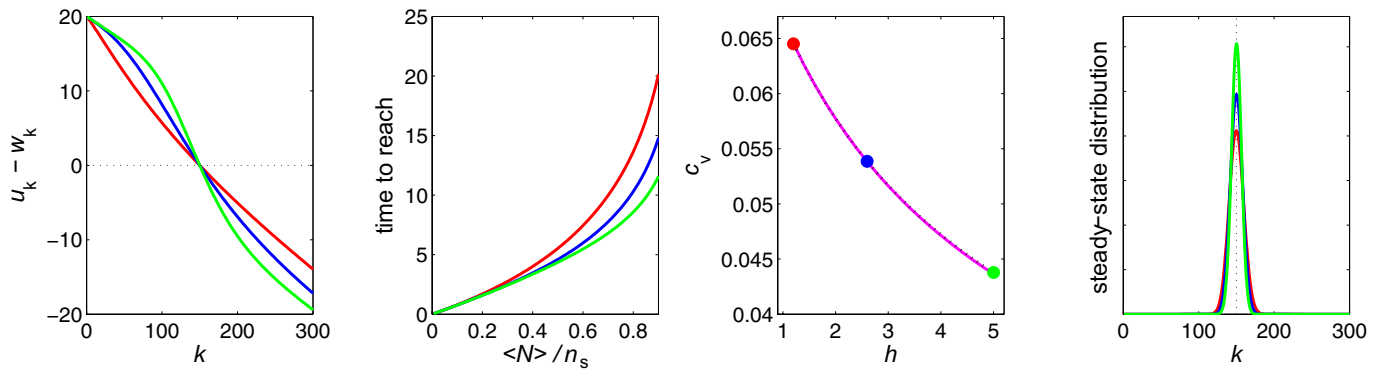


Fig. S7. The same as Fig. S3, but for the model Id.

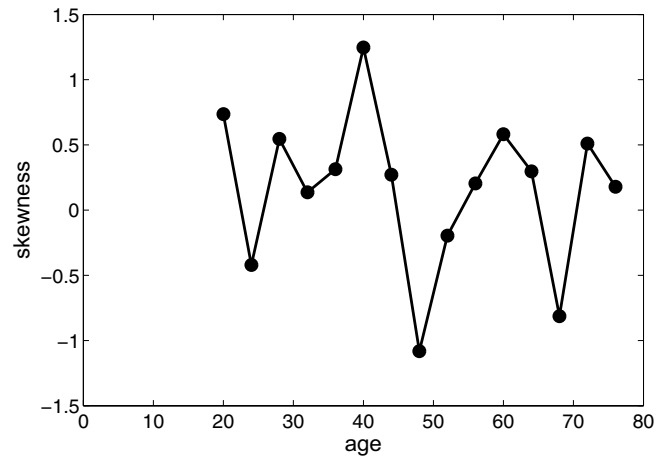
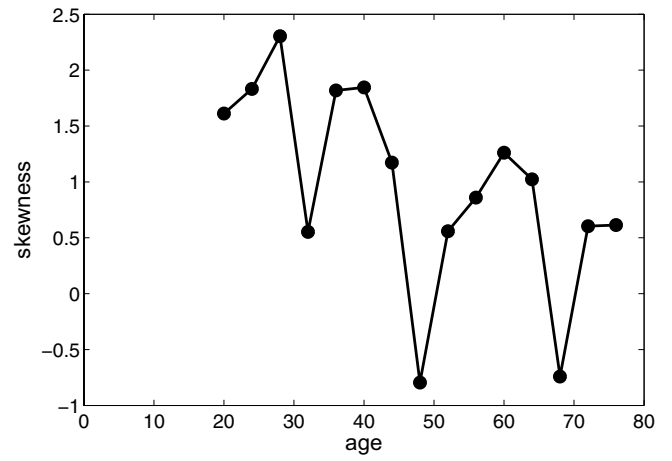
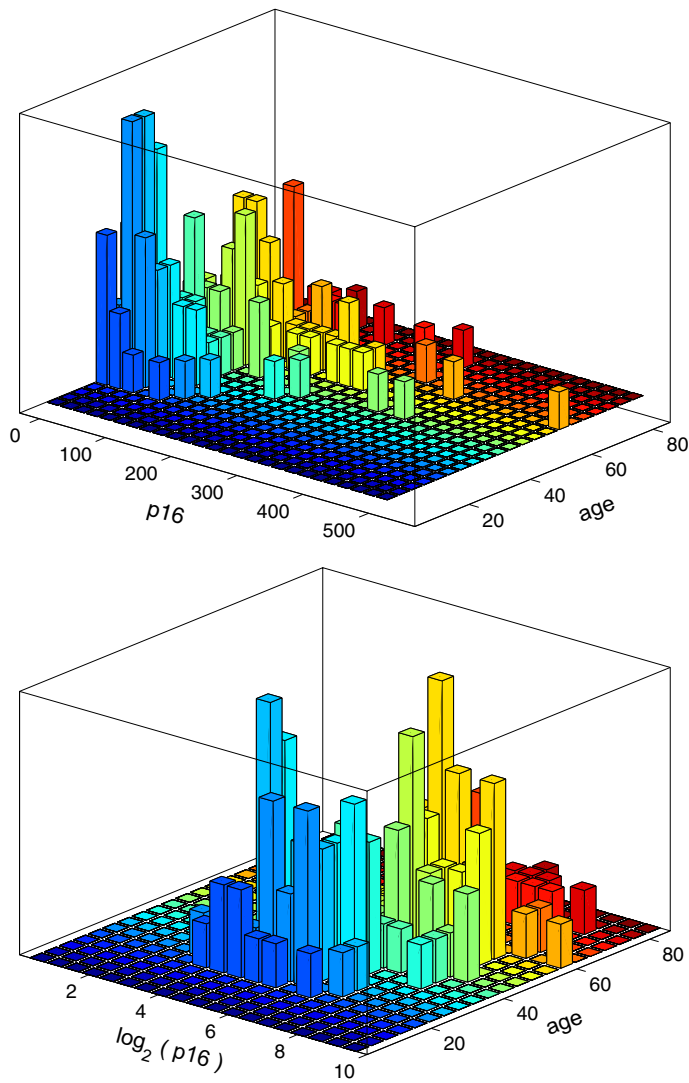


Fig. S8. (Upper) 2D histogram of the data counts generated by fixed 4×20 binning and the corresponding distribution skewness as a function of age. (Lower) The same as Upper, but for the data in \log_2 scale.

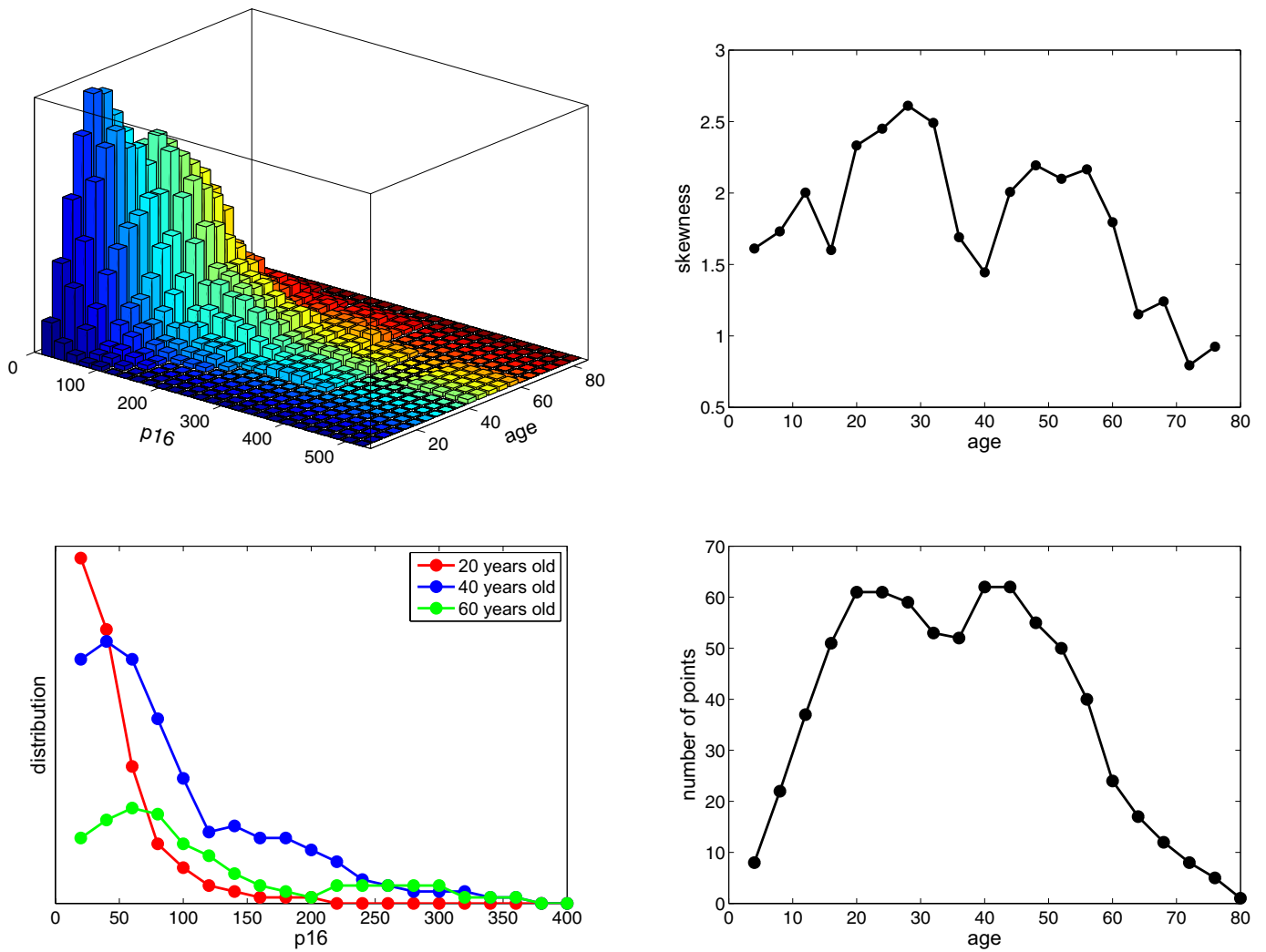


Fig. S9. (Upper) The same as the Upper graphs in Fig. S8, but generated by 20×100 bins moving at 4- and 20-unit steps along "age" and "p16" axes, respectively. (Lower) Data distributions and the number of data points in 4-year slots around 20-, 40-, and 60-year marks.

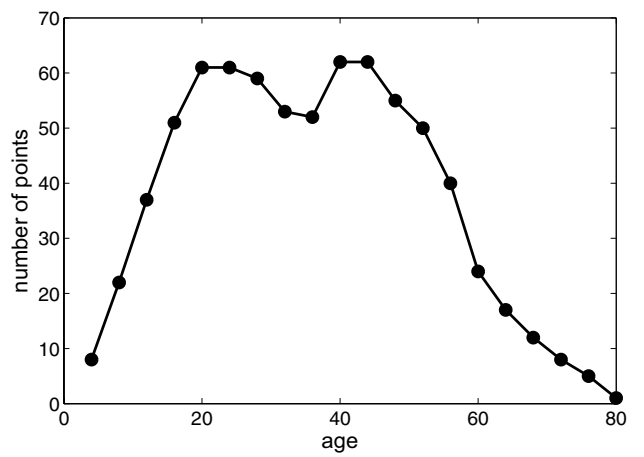
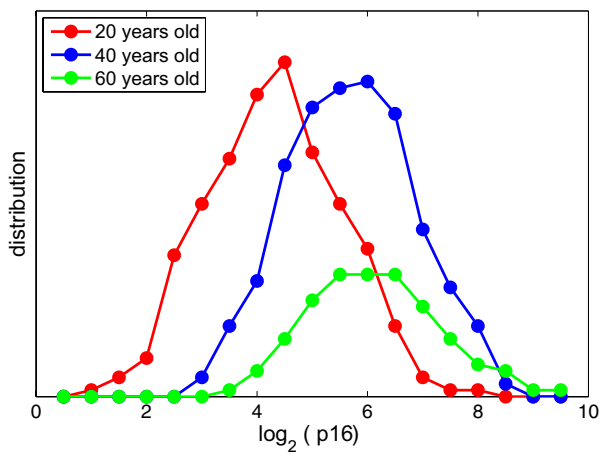
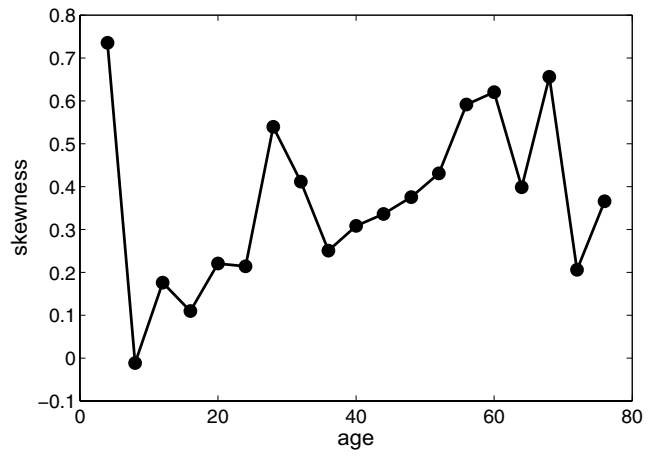
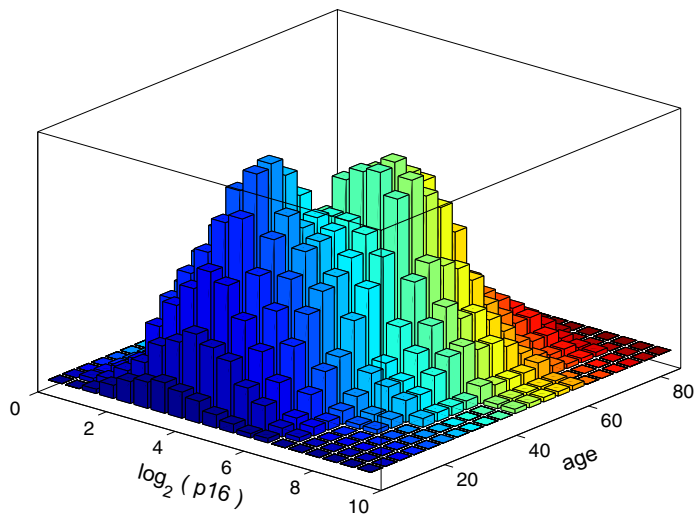


Fig. S10. The same as Fig. S9, but for the data in \log_2 scale.

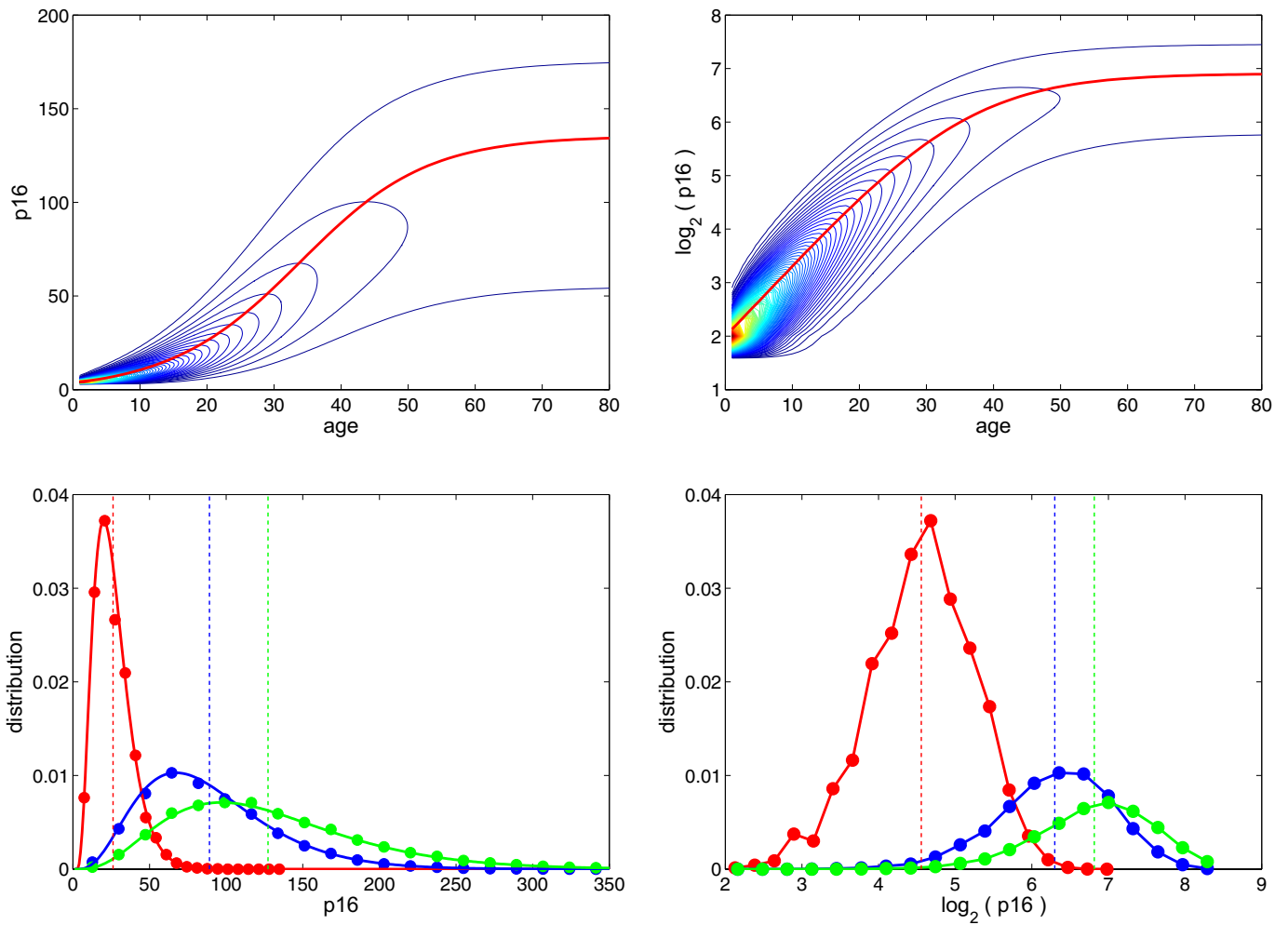


Fig. S11. (Upper) Contour plots of probability distributions (in linear and \log_2 scales) as derived for the model II. (Lower Left) The theoretical probability distribution for 20-year-old (red), 40-year-old (blue), and 60-year-old (green) individuals. (Lower Right) The probability distribution of \log_2 of data generated by the distributions plotted on the Left graph, respectively.

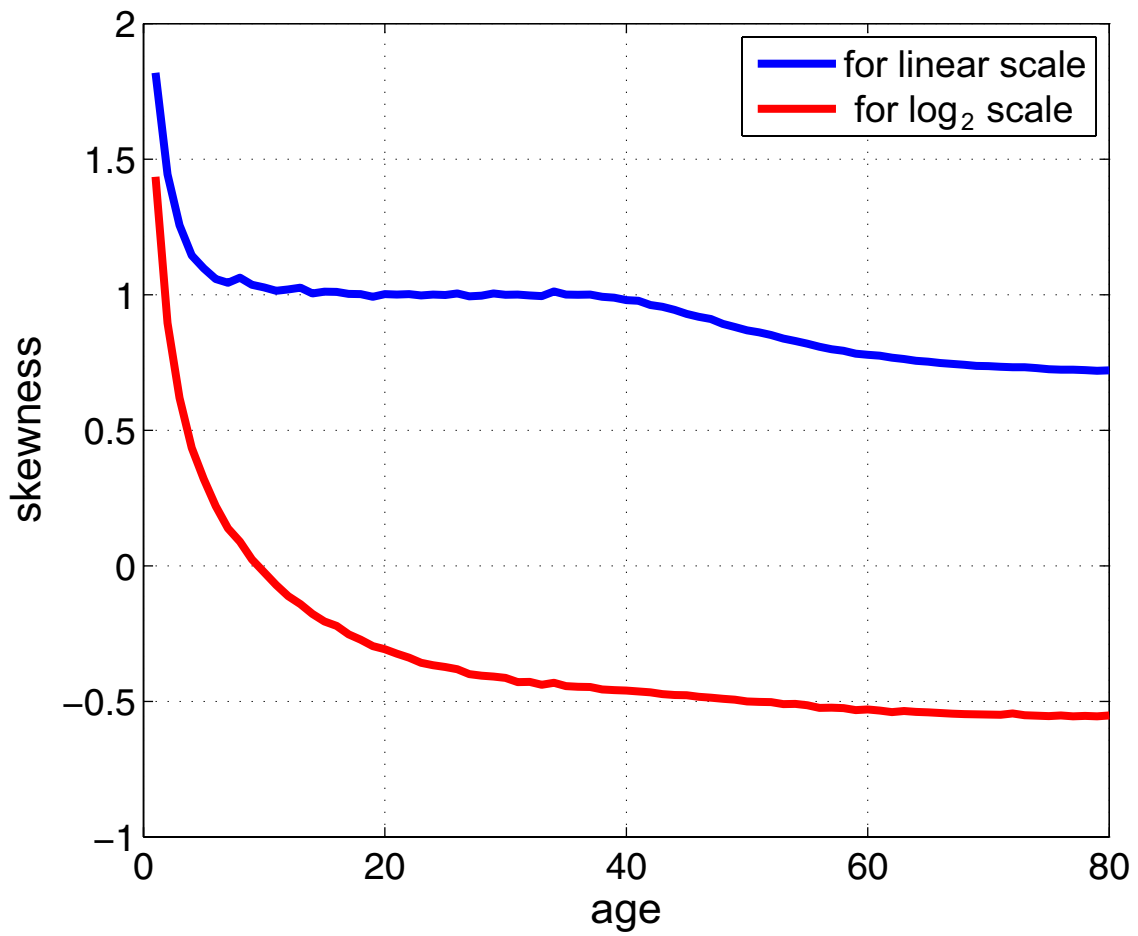


Fig. S12. The skewness of the probability distributions for the model II plotted as a function of age.

Other Supporting Information Files

[SI Appendix \(PDF\)](#)